



Unified constitutive model for granular–fluid mixture in quasi-static and dense flow regimes

Xiaogang Guo¹ · Chong Peng² · Wei Wu² · Yongqi Wang³

Received: 22 June 2020 / Accepted: 18 July 2020 / Published online: 18 September 2020
© Springer-Verlag GmbH Germany, part of Springer Nature 2020

Abstract

Most granular materials encountered in nature and industry lie either in the quasi-static regime or the intermediate dense flow regime. Debris materials are a typical granular material with viscous interstitial fluid and show solid-like behaviors before failure and fluid-like behaviors after failure. Based on Bagnold's pioneering work on granular–fluid flows, we propose a framework for constitutive model development, which has an additive form. Based on this framework, a unified constitutive model for granular–fluid material in the quasi-static and dense flow regimes is developed. The main inter-granular interactions and granular–fluid interactions controlling the mechanical behaviors are taken into account using the Mohr–Coulomb model and a Bagnold-type relation. Dry granular flows in three simple configurations, i.e., plain shear, vertical chute flow and flow on an inclined plane, are studied. Analytical solutions based on the presented unified model are obtained. Comparisons between results from the presented model and the $\mu(I)$ model indicate that the explicit partition of frictional and collisional stress components provides insights into dense granular flows. In addition, the new model is used to predict the stress–strain relations in two annular shear tests. The applicability and advantages of the unified model are discussed.

Keywords Constitutive model · Dense flow regimes · Dynamic viscosity · Granular–fluid flows · Solid volume fraction

1 Introduction

Granular flows are widely presented in industry and nature, e.g., raw material processing and geophysical flows. With different material properties, external loads and boundary conditions, granular materials can behave like solid, fluid or gas. Debris flows are typical granular flows with viscous interstitial fluid which show solid-like behaviors before failure and fluid-like behaviors after failure. They are normally treated as a fluid continuum with microstructural

effect in constitutive modeling for the fluid-like behaviors [12, 13]. However, a constitutive model that can describe both the solid-like and fluid-like behaviors is required for a complete simulation of the process from quasi-static state to the fast flowing state. In the quasi-static regime, the solid-like granular materials can be sufficiently described using plasticity theories in soil mechanics, whereas constitutive equations based on kinetic theory have been proposed for the gas regime [22]. However, most granular flows lie neither in the slowly shearing quasi-static regime, nor in the fully collisional gas regime. In the intermediate flow regime, the granular volume fraction is close to its critical value; thus, the flows can be considered incompressible. This flow regime is usually referred to as dense flow regime in the literature.

In the dense flow regime, the granular material behaves like a liquid dominated by micromechanics of the granular mass [7]. Two distinct features are observed for dense granular–fluid flows. The first is that there exists a threshold yield stress below which the granular media stops flowing; the second is that the granular–fluid flows are

✉ Wei Wu
wei.wu@boku.ac.at

¹ Institute of Geotechnical Engineering, Zhejiang University, Yuhangtang Road 866, Hangzhou 310058, China

² Institute of Geotechnical Engineering, University of Natural Resources and Life Sciences, Vienna, Feistmantelstrasse 4, 1180 Vienna, Austria

³ Department of Mechanical Engineering, Technical University of Darmstadt, Otto-Berndt-Strasse 2, 64287 Darmstadt, Germany

shear rate dependent. These two features arise from three types of dominant interactions in dense granular–fluid flows: frictional contacts and collisions between solid particles, and viscous drag forces between solid particles and the interstitial fluid. The continuously evolving network of frictional contacts results in the frictional behaviors in the dense granular flows, whereas the viscous rate-dependent behavior has its source in the fluid viscosity and the particle collisions. Which interaction is more dominant depends on several factors, e.g., material property, external load and boundary condition.

In a pioneering work on a gravity-free dispersion of solid spheres sheared in Newtonian liquids, which can be considered as a simple shear test shown in Fig. 1, Bagnold [2] proposed a constitutive model in which the shear stress has the relation

$$T_v = 2.25\lambda^{\frac{3}{2}}\mu \frac{dU}{dy} = k_1 \frac{dU}{dy} \quad (1)$$

in the so-called macro-viscous regime and

$$T_i = 0.042\rho_s(\lambda d)^2 \left(\frac{dU}{dy}\right)^2 \sin\alpha_i = k_2 \left(\frac{dU}{dy}\right)^2 \quad (2)$$

in the ‘grain-inertia’ regime, respectively. In the above expressions, μ is the dynamic viscosity of the interstitial fluid; ρ_s and d are the material density and the mean diameter of the grains, respectively; dU/dy denotes the shear strain rate; the tangent of α_i corresponds to the ratio between the shear and normal stress in the grain-inertia regime; λ is the linear concentration defined by

$$\lambda = \frac{d}{s} = \left[\left(\frac{C_0}{C}\right)^{\frac{1}{3}} - 1 \right]^{-1}, \quad (3)$$

where s is the free distance between two particles, C is the mean solid volume fraction, and C_0 is the maximum possible solid volume fraction when $\lambda \rightarrow \infty$ ($s = 0$). In Bagnold’s case, an analytical value for spheres, 0.74, was employed for C_0 . In general cases, the maximum measured

solid volume fractions were found related to the size of the particles and the container dimensions. Usually, C_0 is replaced by the asymptotic limit of the maximum measured solid volume fraction C_∞ as the container dimensions approach infinity [16].

A dimensionless value termed ‘Bagnold number’ is defined as

$$B = \frac{\lambda^{\frac{1}{2}}\rho_s d^2 (dU/dy)}{\mu} \propto \frac{T_i}{T_v} \quad (4)$$

to characterize the granular flow regimes as macro-viscous ($B < 40$), grain-inertia ($B > 450$), or a transitional state ($40 \leq B \leq 450$) between the two limits. The viscosity of the interstitial fluid and the particle collisions are believed to be dominant factor in the macro-viscous regime and grain-inertia regime, respectively.

The normal stress P is observed proportional to the shear stress T with a constant ratio, 0.75, in the macro-viscous region which decreases progressively through the transition region, till reaches another constant value at about 0.32 in the grain-inertia region. It is formulated as

$$\frac{T_v}{P_v} = \tan\alpha_v = 0.75 \quad (5)$$

in the macro-viscous region and

$$\frac{T_i}{P_i} = \tan\alpha_i = 0.32 \quad (6)$$

in the grain-inertia region, where the tangents of α_v and α_i are the stress ratios in different regimes and related to the material properties. In Bagnold’s experiments, the density of the solid particles is equal to that of the interstitial fluids. The effect of gravity was eliminated, and therefore, no yield stress was observed in the experiment. This setup highlights the effect of the fluid viscosity and the particle collisions on the flowing behaviors after failure. The models developed based on the experimental observations never take yield criterion into account and cannot be applied to describe the solid-like behaviors before flowing. In addition, the constitutive relations of (1) and (2) are developed for both the specific flow regimes. The constitutive model for the transition region is unknown, and the two flow regimes are not unified in a constitutive framework. Bagnold’s model cannot achieve a complete description of the stress state in the process from the quasi-static state to the flowing state. The transition between the two flow regimes cannot be investigated consequently.

Another widely accepted constitutive model for dense granular flow regime is the $\mu(I)$ model [19]. It employs an overall phenomenological frictional coefficient related to a dimensionless ‘inertial number.’ Frictional contact and collision are not explicitly considered in this model. Furthermore, as it is developed for dry granular flow, the drag

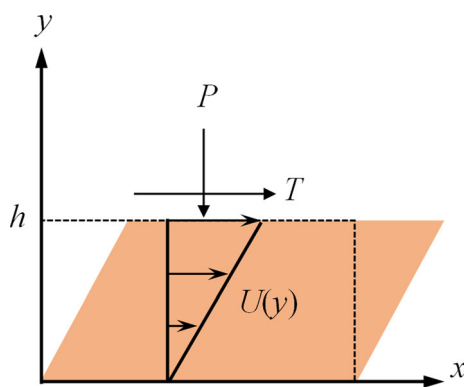


Fig. 1 Schematic of a simple shear test

force imposed on the solid particles by the viscous interstitial fluid is not taken into account. Boyer et al. [6] extended this model to general cases with viscous interstitial fluids. However, the mechanical behaviors inside the yield surface are undefined in both of the models. Thus, the $\mu(I)$ model cannot be applied to granular materials in the quasi-static regime.

This paper aims to develop a framework of constitutive modeling to unify the constitutive theories for the solid-like and fluid-like behaviors of a granular–fluid mixture. A simple-shearing model is developed based on the framework by employing the Bagnold-type relations for the dense flow regimes and the elastoplastic theory, a Mohr–Coulomb-type relation, for the quasi-static regime. The applicability of the Mohr–Coulomb-type relation to describe the solid-like behaviors is discussed. Based on the effort devoted to examine Bagnold’s pioneer work [5, 17, 21, 27], the constitutive relations for the macroviscous and grain-inertia regimes are modified and unified in the new model to consider the dynamic behaviors. It was demonstrated that this framework provides a complete description for granular–fluid materials under slow plastic deforming and fast collisional shearing. In this work, dry granular flows in simple configurations are studied to get analytical solutions based on the presented unified model. The results are compared with the analytical solutions obtained using the $\mu(I)$ model. In addition, the new model is employed to predict the stress–strain relations of two annular shear tests, the numerical and experimental results are compared. The applicability and advantages of the unified model are discussed.

2 Framework of the constitutive model for granular–fluid flows

As pointed out above, the constitutive relations (1) and (2) were developed for two distinct regimes, respectively. The constitutive relation for the transition region is absent so that the continuous description of the flow regimes is impossible. In granular–fluid flows, the intergranular friction, collisions and the fluid viscous force are believed to coexist and transfer momentum simultaneously [18]. Thus, an additive form combining (1) and (2), which reflect the viscous fluid flow and the particle collisions, respectively, is employed for the shear stress of a dense granular–fluid flow. The total rheological shear stress T_r is the sum of T_v and T_i , i.e.,

$$T_r = T_v + T_i. \quad (7)$$

Figure 2 shows the comparison between experimental data and numerical predictions using Eq. (7). It is found that the direct additive form can correctly capture the overall

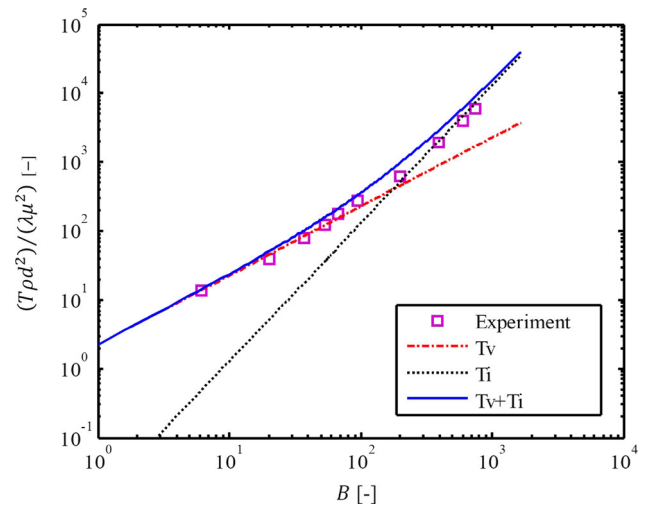


Fig. 2 Comparison between the shear stress predicted by (7) and experimental data of $\lambda = 11$ in [2]

dynamic behavior and provide an easy yet seamless transition. The material parameters introduced in Bagnold’s experiments are used in the stress prediction by combining equations (1) and (2) into (7).

The constitutive relation for the transition regime is therefore determined. As the shear rate increases, the domination of the mechanical behaviors changes from the fluid viscosity to the particle collisions spontaneously in a dense suspension. Likewise, the total rheological normal stress P_r can be described by

$$P_r = P_v + P_i. \quad (8)$$

Ness and Sun [23] proposed a similar constitutive equation based on the additive form combining viscous effects with dry granular rheology. In their equation, the prolonged frictional contact and the particle collisions are not distinguished. The former is believed to be rate independent and cannot be sufficiently described by rate-dependent rheological models. As mentioned before, the yield stress, derived from the prolonged frictional contact, was not accounted for in the Bagnold’s model since the effect of the solid particles’ weight was eliminated in the experiments. For general cases of granular–fluid mixture, the contact friction in the quasi-static regime and residual stresses after failure are essential parts of a complete model. The constitutive equations for granular flows should satisfy a generalized Mohr–Coulomb-type yield criterion as $dU/dy \rightarrow 0$ [9, 25]. Shibata and Mei [27] assumed the following relation for the quasi-static regime

$$T_0 = -fP_0 \operatorname{sgn}\left(\frac{dU}{dy}\right), \quad (9)$$

where T_0 and P_0 are the shear and normal stresses in the quasi-static state; f is an empirical coefficient of dynamic

friction. The ‘sgn’ function is applied to return the sign of the shear strain rate.

The particle weight induced stresses are combined with the rheological stresses by following the additive form to yield a constitutive framework as

$$P = P_0 + P_r = P_0 + P_v + P_i, \quad (10a)$$

$$T = T_0 + T_r = T_0 + T_v + T_i, \quad (10b)$$

where P_0 and T_0 are regarded as the static portion of the framework. T_r and P_r are the dynamic portion. The framework is akin to the assumption of constitutive modeling for granular materials in [29], in which the stress tensor can be decomposed into a static (rate independent) part and a dynamical (rate dependent) part from the perspective of statics. The framework based on the assumption was preliminarily validated in cases of dry granular flow where the viscous terms P_v and T_v are negligible [15, 24]. The constitutive model based on this framework is capable to describe the stress state throughout the shearing process from quasi-static to high-speed shearing stage.

The framework can predict steady uniform flows over a range of bed slopes rather than only for one critical slope for dry granular flows on an inclined plane, which is consistent with the experimental observations [4, 25].

3 Constitutive model for dense granular–fluid flows

In this section, a concrete simple-shearing model for granular–fluid flow is developed based on the framework of (10). A conventional approach is employed to determine the static stresses P_0 and T_0 . The specific expression for the dynamic portion is determined by modifying the Bagnold’s models. Both of the static and dynamic portions are formulated for the solid phase and therefore regarded as effective stress defined in soil mechanics. It is clear that the stresses determined by (1) and (2) will vanish when the solid volume fraction is equal to zero.

3.1 Constitutive relation for quasi-static state

As indicated by equation (9), the yield stress T_0 is proportional to the normal stress P_0 with a constant friction coefficient. The empirical friction coefficient, f , is determined as the tangent of the residual friction angle ϕ since the yield stress is assumed equal to the residual stress in the Mohr–Coulomb-type relation. The friction angle can be obtained in simple shear tests [26] and is assumed independent of the shear rate. From (9), the shear stress in quasi-static stage is expressed as

$$T_0 = -P_0 \operatorname{sgn}\left(\frac{dU}{dy}\right) \tan \phi. \quad (11)$$

Once P_0 is determined, the shear stress T_0 will be obtained consequently. The normal stress P_0 usually stems from the gravity of the solid particles.

Take the free surface granular–fluid flow shown in Fig. 3 as an example, the normal stress is the component of gravity perpendicular to the flow plane,

$$P_0 = (\rho_s - \rho_f)Cgh\cos\theta, \quad (12)$$

where ρ_f is the density of the fluid. It is worth to mention that the normal stress determined by (12) is considered as the initial value of P_0 . The static stress P_0 will decrease with the increase in shear rate in the dense flow regime since more fierce particle collisions lead to less prolonged contact.

The simple relation (11) is widely employed as it is easy to be understood and implemented in numerical calculations. The expression (12) was proved applicable in the cases without shear softening (or liquefaction in saturated granular material) in the quasi-static state [20]. For the cases with excess pore pressure, more complicated constitutive theories are required for the quasi-static regime. It is stated that granular materials show rate-independent hypoplastic behaviors under monotonous deformations [14].

3.2 Constitutive relations for dense flow regime

From (1) and (2), together with (4), two dimensionless quantities are obtained as

$$\frac{T_v \rho_s d^2}{\lambda \mu^2} = 2.25B \quad (13)$$

and

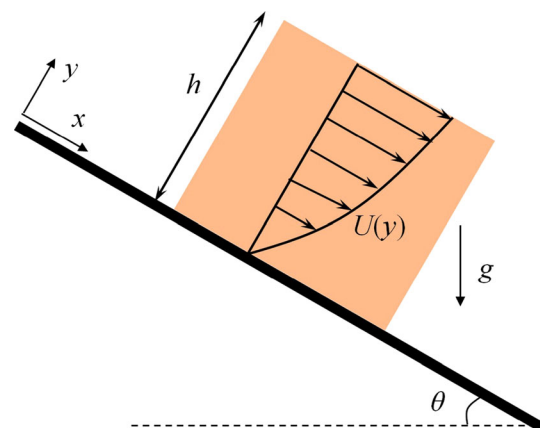


Fig. 3 Schematic of a steady granular–fluid flow on an inclined plane

$$\frac{T_i \rho_s d^2}{\lambda \mu^2} = (0.042 \sin \alpha_i) B^2, \tag{14}$$

which depend only on the Bagnold number B . These relationships cannot describe the experimental observations when the linear concentration, λ , is greater than 12 [2, 17]. It implies that the dimensionless quantities are also dependent on the linear concentration. Thus, the dimensionless quantities are extended to the following general expressions as

$$\frac{T_v \rho_s d^2}{\lambda \mu^2} = f_1(\lambda) B \tag{15}$$

and

$$\frac{T_i \rho_s d^2}{\lambda \mu^2} = f_2(\lambda) B^2, \tag{16}$$

where $f_1(\lambda)$ and $f_2(\lambda)$ are functions of λ to be specified.

3.2.1 (a) Shear stress in the macro-viscous regime

The shear stress in the macro-viscous regime is first investigated with the goal to find a constitutive model applicable in the whole spectrum of λ studied in Bagnold’s experiments. For the viscous regime, Bagnold derived the expression of total shear stress as

$$\bar{T}_v = (1 + \lambda) \left[1 + \frac{1}{2} f(\lambda) \right] \mu \frac{dU}{dy}, \tag{17}$$

in which \bar{T}_v is the total shear stress consisting of the contributions of grain and fluid, T_v and τ_v ; $f(\lambda)$ is a function of the linear concentration and reflects the amplitude of the shear velocity fluctuation, and $f(0) = 0$. In order to determine the shear stress of the solid phase, the total shear stress needs to be divided into T_v and τ_v . Bagnold assumed a simple relation for the fluid contribution in the total shear stress in the grain-inertia regime as [3, 17]

$$\tau_i = \frac{\tau_0}{(1 + \lambda)}, \tag{18}$$

where τ_0 is the shear stress in pure fluid and formulated as $\mu dU/dy$. The fluid contribution decreases as the linear concentration increases. This relation is assumed to hold in the macro-viscous regime as well. Thus,

$$\tau_v = \frac{\mu}{(1 + \lambda)} \frac{dU}{dy}. \tag{19}$$

Based on (17) and (19), the contribution of grain is derived as

$$T_v = \bar{T}_v - \tau_v = \left\{ (1 + \lambda) \left[1 + \frac{1}{2} f(\lambda) \right] - \frac{1}{1 + \lambda} \right\} \mu \frac{dU}{dy}. \tag{20}$$

Bagnold employed $f(\lambda) = \lambda$ in (17). Thus, the expression of T_v is preliminarily determined as

$$T_v = \left[(1 + \lambda) \left(1 + \frac{1}{2} \lambda \right) - \frac{1}{1 + \lambda} \right] \mu \frac{dU}{dy}. \tag{21}$$

The dimensionless quantity derived from (21) is

$$\frac{T_v \rho_s d^2}{\lambda \mu^2} = \left(\lambda^{-\frac{3}{2}} + \frac{3}{2} \lambda^{-\frac{1}{2}} + \frac{1}{2} \lambda^{\frac{1}{2}} + \frac{\lambda^{-\frac{3}{2}}}{1 + \lambda} \right) B, \tag{22}$$

which demonstrates a concrete formula of the proposition of (15). The model (21) is capable to predict the experimental results for granular–fluid mixture with high concentration to some extent. For exact prediction, a further modification is needed.

A well-known phenomenon in granular–fluid flows is that the shear stress is relatively insensitive to the solid volume fraction C when the value of C is below approximately 0.5, but increases rapidly when the solid volume fraction exceeds this critical value [16]. Some researchers [11, 28] used a power series of the volume fraction (or the linear concentration) combined with an exponential term to describe the dynamic viscosity of granular–fluid mixture. These expressions were determined by fitting shear stress versus shear strain rate curves. The mechanism of the phenomenon needs further clarification. As pointed out by Bagnold [2] and Hanes and Inman [16], the solid volume fraction must be less than a critical value C_c to assure a full shearing to occur. The critical value was found to depend on the packing pattern and lay between 0.53 and 0.65 [3, 27]. For the general case of a gravity flow shown in Fig. 4, a stagnant zone with thickness of $H - h$ will arise at the bottom of the specimen when the mean solid volume fraction C is greater than C_c . If the total thickness H rather than that of the flowing zone h is used in the calculation of the shear strain rate, an underestimated result will be obtained. In a steady flow with $C > C_c$, the exchange of particles between the flowing and the stagnant zone reaches a balance. The mean solid volume fraction in the upper layer, C_f , is deduced to be unchanged as the critical value

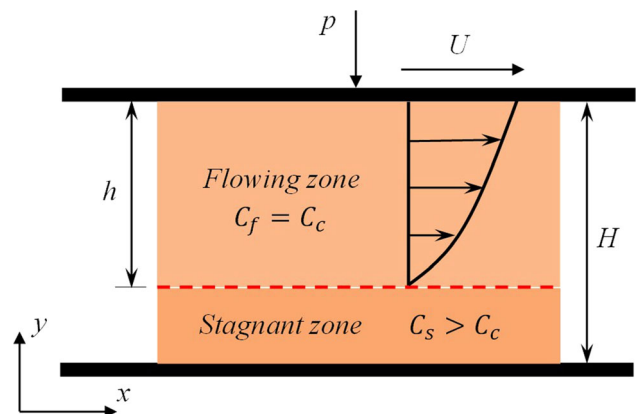


Fig. 4 Schematic of a simple-shearing granular–fluid flow with a stagnant zone

C_c . The mean value of the stagnant zone C_s should be greater than C_c to keep static. Otherwise, solid particles will move from the stagnant zone to the flowing zone till C_f reaches the value of C_c . Thus, the experimental observation that the shear stress increases dramatically when the solid volume fraction exceeds the critical value C_c is attributed to both the increase in the dynamic viscosity and the decrease in the thickness of the flowing zone. Therefore, the critical value of solid volume fraction should be taken into account in the simple-shearing model for dense granular–fluid flow. Inspired by the way to take the critical value into account in [27], the following model is proposed for the macro-viscous regime.

$$T_v = K_1 \frac{dU}{dy}, \tag{23}$$

where

$$K_1 = \left[(1 + \lambda) \left(1 + \frac{1}{2} \lambda \right) - \frac{1}{1 + \lambda} \right] \mu \left(1 - \frac{C}{C_c} \right)^{-n} \tag{24}$$

is called effective viscosity; n is a fitting parameter. In Shibata and Mei’s work [27], it was chosen $n = 1$.

3.2.2 (b) Shear stress in the grain-inertia regime

The constitutive equation for the grain-inertia regime is slightly modified based on Equation (16). The experimental results in [2] show that shear stresses in different regimes deviate as a whole with the change of the linear concentration in the logarithm coordinates of $\rho_s d^2 (dU/dy)^2$ versus grain shear stress. It is assumed that the shear stress T_i changes in the same rate with T_v when the value of λ varies. Based on this assumption, the original equation for the ‘grain-inertia’ regime, (2), is modified to be

$$T_i = K_2 \left(\frac{dU}{dy} \right)^2, \tag{25}$$

where

$$K_2 = 0.042 R_v \rho_s (\lambda d)^2 \sin \alpha_i \tag{26}$$

and

$$R_v = \frac{K_1}{k_1} = \frac{\left[(1 + \lambda) \left(1 + \frac{1}{2} \lambda \right) - \frac{1}{1 + \lambda} \right] \left(1 - \frac{C}{C_c} \right)^{-n}}{2.25 \lambda^{\frac{3}{2}}} \tag{27}$$

is termed as correction factor.

3.3 A simple-shearing model for dense granular–fluid mixture

Substituting (23) and (25) into (7) yields the expression of shear stress in the dense flow regime

$$T_r = K_1 \frac{dU}{dy} + K_2 \left(\frac{dU}{dy} \right)^2. \tag{28}$$

Based on (5), (6) and (8), the normal stress in the flowing state is expressed as

$$P_r = \frac{K_1}{\tan \alpha_v} \frac{dU}{dy} + \frac{K_2}{\tan \alpha_i} \left(\frac{dU}{dy} \right)^2. \tag{29}$$

The modified models are capable of describing the mechanical behaviors of a dense granular–fluid mixture from the ‘macro-viscous’ regime to the ‘grain-inertia’ regime. As shown in Fig. 5, by choosing $n = 0.2$ and $C_c = 0.65$ [16], (28) and (29) can predict Bagnold’s experimental results with satisfactory agreement.

Furthermore, based on the framework (10), the dynamic stresses (28) and (29) are combined with the static stresses T_0 and P_0 , respectively, to obtain a simple-shearing model as

$$P = P_0 + \frac{K_1}{\tan \alpha_v} \frac{dU}{dy} + \frac{K_2}{\tan \alpha_i} \left(\frac{dU}{dy} \right)^2, \tag{30a}$$

$$T = -P_0 \operatorname{sgn} \left(\frac{dU}{dy} \right) \tan \phi + K_1 \frac{dU}{dy} + K_2 \left(\frac{dU}{dy} \right)^2. \tag{30b}$$

This is a simple example of the unified model for granular–fluid mixture in the quasi-static and dense flow regimes. The rate-independent constitutive component for the unified model can be chosen according to the requirement in comprehensively modeling the behaviors inside the yield surface.

4 Analytical solutions for steady granular flows

Three dry granular flows under simple configurations are studied. Analytical solutions from the simple-shearing model are compared to the solutions from the $\mu(I)$ model.

4.1 Plane shear flow

Consider shearing of a granular material made of particles with diameter d and density ρ_s , as shown in Fig. 1. The confining pressure P is imposed on the top plate. The granular material is sheared at a prescribed rate $\dot{\gamma} = U/h$, where U is the velocity of the top plate and h is the depth of the granular body. Gravity is not considered. To maintain a steady plane shear, the shear force on the top plate depends on the imposed confining pressure and shear rate.

In the $\mu(I)$ model, the inertial number can be calculated through

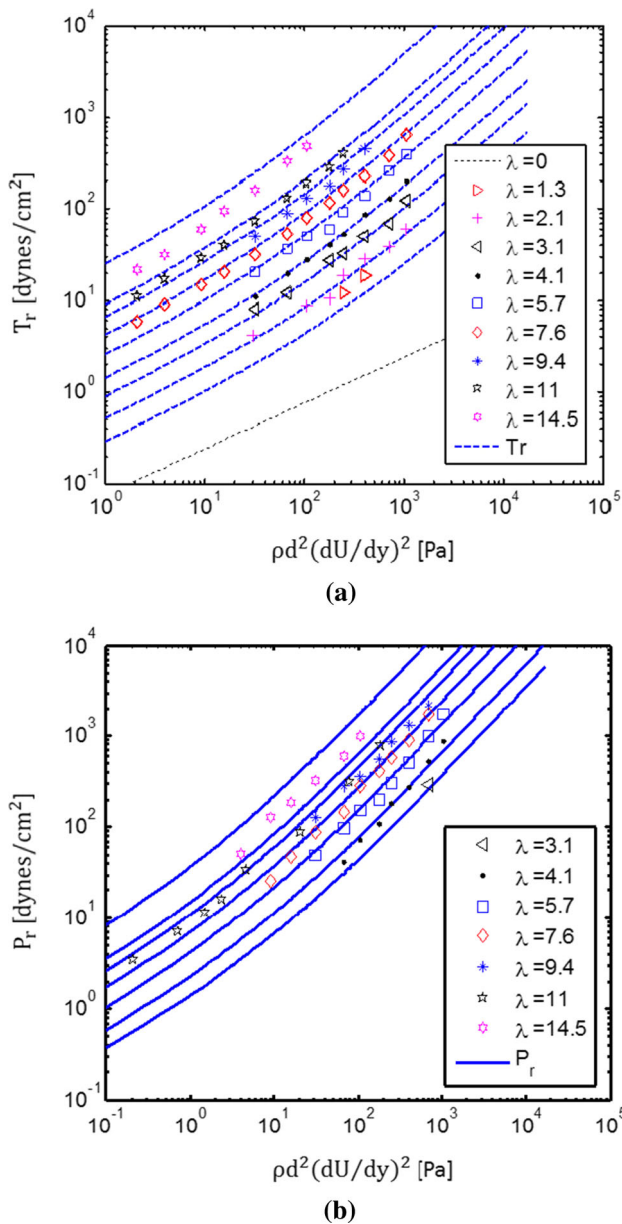


Fig. 5 Comparison between the stresses predicted by (28) and (29) with $n = 0.2$ and $C_c = 0.65$ and the data from **a** the figure 3 and **b** the figure 4 in [2]. The experimental data are indicated by various symbols. The dashed lines (upper panel) denote the shear stresses, while the solid lines (lower panel) are the normal stresses

$$I = \frac{d\dot{\gamma}}{\sqrt{P/\rho_s}} \tag{31}$$

Consequently, we can obtain the shear stress T by [19]

$$T = \mu(I)P, \text{ with } \mu(I) = \mu_1 + \frac{\mu_2 - \mu_1}{I_0/I + 1}, \tag{32}$$

where μ_1, μ_2 and I_0 are three parameters of the $\mu(I)$ model.

With the presented unified model, considering the steady shearing of dry granular materials where the viscous

terms are negligible, we have the following two expressions

$$T = \sigma_{yy}^f \sin \phi + K_2 \dot{\gamma}^2, \tag{33}$$

and

$$P = \sigma_{yy}^f + \frac{K_2}{\tan \alpha_i} \dot{\gamma}^2. \tag{34}$$

The frictional shear stress is computed as $\sigma_{yy}^f \sin \phi$, instead of $\sigma_{yy}^f \tan \phi$, because simulations of plane shear flows indicate that the difference between the vertical and the horizontal normal stress is very small, i.e., $\sigma_{xx}^f \approx \sigma_{zz}^f$ [1, 10]. The frictional shear stress is then equal to $\sigma_{yy}^f \sin \phi$. Based on Eqs. (33) and (34), the total shear force is obtained as

$$T = P \sin \phi + K_2 \dot{\gamma}^2 \left(1 - \frac{\sin \phi}{\tan \alpha_i} \right). \tag{35}$$

Comparing Eqs. (32) and (35), it can be observed that the shear stresses obtained by using the $\mu(I)$ model and the unified model have a similar structure. Both results consist of two parts, one part is constant with given normal stress P , and the other one depends on the shear rate. In the dense flow regime, the shear stress obtained using the $\mu(I)$ model ranges from $\mu_1 P$ to $\mu_2 P$. On the other hand, in the dense flow regime, the dispersive pressure $P_i = K_2 \dot{\gamma}^2 / \tan \alpha_i$ is from 0 to P ; therefore, the range of shear stress obtained using the unified model is from $P \sin \phi$ to $P \tan \alpha_i$. It is observed that the constants $\sin \phi$ and $\tan \alpha_i$ in the unified model are equivalent to the constants μ_1 and μ_2 in the $\mu(I)$ model.

Both of the models enable precise classifications of the three flow regimes of dry granular materials: quasi-static, dense flow and gaseous. Small values of $\dot{\gamma}$ ($\dot{\gamma} \rightarrow 0$) correspond to the quasi-static regime in the sense that deformation is very slow. In the $\mu(I)$ model, the threshold of I corresponds to the rapid and dilute flow regime is $I \approx 1$, which is obtained from experiments [1]. Contrarily, in the unified model, the gaseous regime can be theoretically determined: it corresponds to the state when the network of frictional contacts disappears, that is, when $\sigma_{yy}^f = 0$. Based on the aforementioned analysis, the shear rate corresponds to the dense flow regime in the plane shear is

$$\begin{aligned} \text{for the } \mu(I) \text{ model : } & 0 < \dot{\gamma} \lesssim \sqrt{P}/\sqrt{\rho_s d^2}, \\ \text{for the unified model : } & 0 < \dot{\gamma} < \sqrt{P}/\sqrt{K_2}. \end{aligned} \tag{36}$$

Again, the ranges of shear rate corresponding to the dense flow regime obtained using the $\mu(I)$ model and the unified model have similar form. Note that the constant K_2 is related to particle diameter, density and solid volume fraction. It can be observed that in both of the models, the

upper limits of the shear rate depend on the confining pressure P and physical properties of the granular material.

Although these two models bear some similarities, there are fundamental differences. The $\mu(I)$ model employs an inertial-number-dependent phenomenological frictional coefficient, which changes with shear rate and confining pressure. However, the model does not give any clue why the phenomenological frictional coefficient $\mu(I)$ changes with different shear rate and confining pressure. On the other hand, the unified model explicitly considers the origin of different stress components. In the unified model, the change of phenomenological frictional coefficient can find its explanation as follows. The ratio between shear stress and normal stress in the network of frictional contacts is related to the internal friction angle ϕ of the material, whereas the ratio of the collision-induced shear/normal stresses is related to another angle α_i . Experiments show that α_i is generally larger than ϕ . Therefore, when the flow state moves from the quasi-static regime to the gaseous regime, the collision-induced stresses become more and more significant. In this process, the phenomenological frictional coefficient increases from $\sin \phi$ to $\tan \alpha_i$. The evolution of the phenomenological frictional coefficient in the two models is written, respectively, as

$$\begin{aligned} \text{in the } \mu(I) \text{ model : } \mu &= \mu_1 + \frac{\dot{\gamma} d (\mu_1 - \mu_2)}{I_0 \sqrt{P/\rho_s} + \dot{\gamma} d}, \\ \text{in the unified model : } \mu &= \sin \phi + \frac{\dot{\gamma}^2 K_2 (\tan \alpha_i - \sin \phi)}{P \tan \alpha_i}. \end{aligned} \quad (37)$$

Comparing Eq. (37) with Eq. (32), the evolutions of the phenomenological frictional coefficient in the two models have a similar structure, but different dependences on shear rate and confining pressure.

4.2 Vertical chute flow

Consider a granular material flowing between two vertical plates with a distance of $2W$, as shown in Fig. 6. The confining pressure on the two vertical plates is P , which implies that $\sigma_{xx} = P$ within the flow in the steady state.

According to the unified model, the possible range of shear stress τ_{xy} in the chute flow is from $P \sin \phi$ to $P \tan \alpha$. Because of symmetry, the shear stress at the center of the flow is zero. Based on the force balance along the x axis, the shear stress can be written as

$$\tau_{xy} = \rho g x, \quad (38)$$

where ρ is the bulk density of the granular material. The steady flow condition requires that the shear stress increases linearly from the flow center to the vertical plates. Consequently, there exists an unsheared zone in

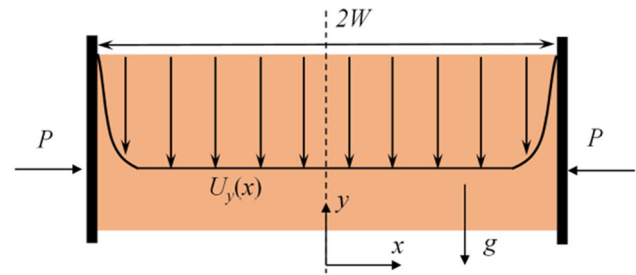


Fig. 6 Schematic of vertical chute flow

which $\tau_{xy} < P \sin \phi$. Namely, when $x < x_p$ ($x_p = P \sin \phi / \rho g$), the granular material is unyielded and moves as a plug layer. If $x_p > W$, the whole granular body is unyielded and no granular flow is possible. Furthermore, the maximum shear stress required for the force balance does not exceed the maximum shear stress that can be provided, i.e., $\tau_{xy} < P \tan \alpha_i$. Therefore, according to the unified model, a steady granular flow is possible in the vertical chute only if

$$\rho g W / \tan \alpha_i < P < \rho g W / \sin \phi. \quad (39)$$

Now we proceed to derive the velocity profile of the steady flow. The stress components for the present vertical chute flow, as specified in (33) and (34) for the plane shear flow, take the forms

$$\begin{aligned} P &= \sigma_{xx}^f + \frac{K_2}{\tan \alpha_i} \left(\frac{dU_y}{dx} \right)^2, \\ \tau_{xy} &= \sigma_{xx}^f \sin \phi + K_2 \left(\frac{dU_y}{dx} \right)^2. \end{aligned} \quad (40)$$

Substituting Eq. (40) into Eq. (38), we have

$$\left(\frac{dU_y}{dx} \right)^2 = \frac{(\rho g x - P \sin \phi) \tan \alpha_i}{K_2 (\tan \alpha_i - \sin \phi)}. \quad (41)$$

Solving the above equation using the boundary condition $U_y = 0$ at $x = W$, we can obtain the velocity profile

$$\begin{aligned} U_y(x) &= U_y^p + \frac{2\sqrt{\tan \alpha_i} (\rho g x - P \sin \phi)^{3/2}}{3\sqrt{K_2} (\tan \alpha_i - \sin \phi) \rho g} \quad \text{if} \\ &x_p \leq x \leq W, \end{aligned} \quad (42)$$

where U_y^p is the velocity of the unsheared plug layer

$$U_y^p = - \frac{2\sqrt{\tan \alpha_i} (\rho g W - P \sin \phi)^{3/2}}{3\sqrt{K_2} (\tan \alpha_i - \sin \phi) \rho g} \quad \text{if } x < x_p. \quad (43)$$

Analytical solutions can also be obtained using the $\mu(I)$ model [8]. Similarly, an unsheared plug layer exists, and there is a confining pressure range, only with confining pressure in this range a steady granular flow is possible. If the parameters in the $\mu(I)$ model are taken as $\mu_1 = \sin \phi$

and $\mu_2 = \tan \alpha_i$, the width of the plug layer and the range of the confining pressure are identical to those obtained from the unified model. However, the velocity profiles obtained using these two models are not identical.

To quantitatively compare the solutions obtained using these two models, the velocity profiles are calculated. The following material properties are used: $\rho = 1470 \text{ kg/m}^3$, $\rho_s = 2450 \text{ kg/m}^3$ and $d = 0.002 \text{ m}$. The parameters for the $\mu(I)$ model are chosen as $\mu_1 = 0.38$, $\mu_2 = 0.64$ and $I_0 = 0.279$. For the unified model, we take $\sin \phi = \mu_1$, $\tan \alpha = \mu_2$ and $K_2 = 0.2$. The width of the chute is 0.2 m, the confining pressure P is 3000 Pa. Owing to the symmetric geometry, only the right half of the granular material is considered. The calculated results are shown in Fig. 7. Using the given parameters, the two models predict identical unsheared velocity. However, the velocity profiles in the shear zone are somewhat different.

4.3 Flow on an inclined plane

The problem of a granular mass on an incline is considered. As shown in Fig. 3, the granular mass has a free surface and is subjected to gravity. The inclination angle is θ . The height of the granular layer is h .

For this steady granular flow, the stress distribution should be hydrostatic

$$\sigma_{yy} = \rho g(h - y) \cos \theta, \sigma_{xy} = \rho g(h - y) \sin \theta. \tag{44}$$

For an infinite inclined plane, we assume that the frictional stresses $\sigma_{yy}^f = \sigma_{xx}^f$ in the flowing state; thus, the shear/normal stress ratio of the frictional contacts is $\tau_{xy}^f/\sigma_{yy}^f = \sin \phi$.

The following force balance must be satisfied in the steady state

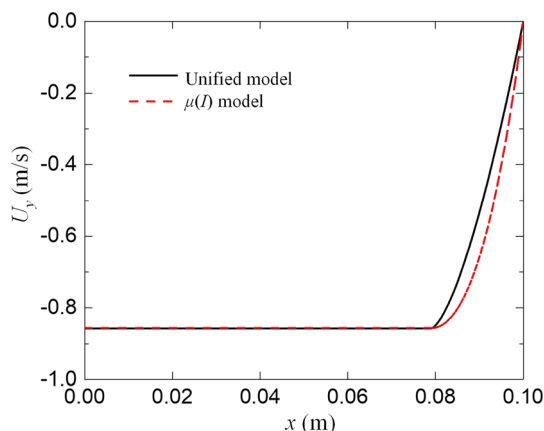


Fig. 7 Velocity profiles obtained using the unified model and the $\mu(I)$ model in the vertical chute flow

$$\begin{aligned} \sigma_{yy} &= \rho g(h - y) \cos \theta = \sigma_{yy}^f + \frac{K_2}{\tan \alpha_i} \left(\frac{dU}{dy} \right)^2, \\ \tau_{xy} &= \rho g(h - y) \sin \theta = \sigma_{yy}^f \sin \phi + K_2 \left(\frac{dU}{dy} \right)^2. \end{aligned} \tag{45}$$

Here, once again, the stress consists of the contributions from frictional contacts and collisions, described by the Mohr–Coulomb model and the Bagnold-type rheology, respectively. Based on the force balance equations, the following differential equation is derived

$$\begin{aligned} (1 - \sin \phi / \tan \alpha_i) K_2 \left(\frac{dU}{dy} \right)^2 \\ - \rho g(\sin \theta - \cos \theta \sin \phi)(h - y) = 0. \end{aligned} \tag{46}$$

Solving the above equation, the velocity profile is obtained as

$$U(y) = \frac{2}{3} \sqrt{\frac{\rho g(\sin \theta - \cos \theta \sin \phi)}{(1 - \sin \phi / \tan \alpha_i) K_2}} (h^{3/2} - (h - y)^{3/2}). \tag{47}$$

The velocity profile, evolving as $(h - y)^{3/2}$, corresponds to the Bagnold profile. Once the velocity is obtained, the stress components from frictional contacts and collisions can be determined. From the velocity profile, it is noted that velocity and shear rate increase with the inclination θ . With increasing θ , the normal and shear stresses induced by collisions become more significant. This increase in the dispersive normal stress results in a trend of dilation, tending to reduce the stress components caused by frictional contacts.

If the granular material is modeled using the $\mu(I)$ model, dense granular flow can only happen if the inclination θ is between $\tan^{-1} \mu_1$ and $\tan^{-1} \mu_2$. With the unified model, a similar inclination range can be derived as follows

$$\tan \theta = \frac{\tau_{xy}}{\sigma_{yy}} = \sin \phi + \frac{\sigma_{zz}^c}{\sigma_{zz}} (\tan \alpha_i - \sin \phi), \tag{48}$$

where σ_{zz}^c is the dispersive normal stress. The steady dense flow condition requires $0 < \sigma_{zz}^c < \sigma_{zz}$, because if $\sigma_{zz}^c > \sigma_{zz}$ the network of frictional contacts disappears completely, which means that the granular material enters the gaseous regime. Consequently, according to the unified model, the inclination range for dense granular flow is

$$\tan^{-1}(\sin \phi) < \theta < \alpha_i, \tag{49}$$

which is exactly the inclination range derived from the $\mu(I)$ model. It is easily seen that the obtained velocity profile is valid only under the condition (49).

The velocity profiles of the granular flow with two different inclinations are calculated. The material parameters used in the calculation are the same as those used in the

former vertical chute flow. For the unified model, the parameters are taken as $\sin \phi = \mu_1 = 0.38$ and $\tan \alpha_i = \mu_2 = 0.64$. Figure 8 shows the results obtained using $K_2 = 0.3$ for $\theta = 23^\circ$, and $K_2 = 0.1$ for $\theta = 25^\circ$. Using the given parameters, the two models provide similar predictions.

5 Performance of the proposed model

In this section, the performance of the unified simple shear model is demonstrated by modeling two tests, respectively, for a dry granular flow and a granular–fluid mixtures flow.

5.1 Case 1: Dry granular materials

The experimental results of dry granular materials sheared in an annular shear cell were reported by Savage and Sayed [26]. In the experiments, the shear velocity was adjusted to keep the height of the granular mass constant and thus keep the volume unchanged. This steady state is equivalent to an undrained simple shear of saturated granular materials. The experimental data for 1.0 mm spherical polystyrene beads are predicted by the new model. The shear stresses were measured on the top surface of the sample. As stated in [26], the loads applied by the upper disk range from 100 to 1500 N/m². However, the specific load for each single sample was not reported. By checking the measured normal stress for 1.0 mm beads, we assume that the normal stress in the quasi-static regime P_0 has a value around 100 N/m² which is also regarded as the residual normal stress after yielding. As mentioned before, the theoretical maximum value of solid volume fraction, C_0 , will be replaced by the asymptotic limit of the maximum measured solid volume fraction, C_∞ , in the calculation for a specific experiment. Since the exact value of C_∞ was not reported in Savage

and Sayed's work, we use 0.65 which is a typical value for monosized spheres [3, 16]. The critical volume fraction C_c is approximately 0.62 [27]. All the parameters for the prediction are listed in Tables 1 and 2.

As shown in Fig. 9, the predicted curves can fit the experimental data at high shear strain rate very well. For the dense specimen, the non-quadratic dependence of the stresses on the shear rate in the slow shear stage is also captured by the new model. However, the predicted results for the specimens with $C < 0.524$ show a slight overestimation, especially in the slow shear stage. The assumed value of P_0 , 100 N/m², is believed to be greater than the real value of the tests with $C < 0.524$. However, as mentioned before, $P_0 = 100$ N/m² is the minimum value which can be imposed on the specimens by the upper disk. A plausible explanation is that shear softening occurs in the relatively loose specimens under undrained condition. In this case, the normal stress P_0 which corresponds to the effective stress in soil mechanics would decrease to a residual value to eliminate the tendency of volume compression. A looser specimen will present lower residual strength. The Mohr–Coulomb-type relations (11) and (12), used as the static portion of (30), cannot capture the decrease in P_0 in the quasi-static stage. However, the dynamic portion is validated in the describing of the stress–strain rate relations for dry granular flows with different solid volume fraction.

5.2 Case 2: Granular–water mixture

Another elementary modeling by the unified simple-shearing model is based on the laboratory tests from Hanes and Inman [16] with spherical particles sheared in water. The data for particles with diameter of 1.85 mm are selected since they are claimed to be of good quality. The

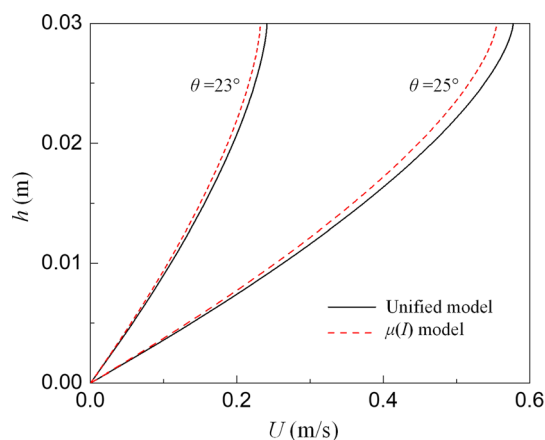


Fig. 8 Velocity profiles obtained using the unified model and the $\mu(I)$ model in the flow on inclined plate

Table 1 Parameters for the shear tests of 1.0 mm beads in [26]

d (mm)	C_∞ (–)	C_c (–)	ρ_s (kg/m ³)	ρ_f (kg/m ³)	μ (Pa s)	ϕ (°)	θ (°)
1.0	0.65	0.62	1095	1.29	1.83×10^{-5}	23	0

Table 2 Stress ratios measured in the shear tests of 1.0 mm beads in [26]

C (–)	$\tan \alpha_v$ (–)	$\tan \alpha_i$ (–)
0.461	0.50	0.51
0.483	0.40	0.51
0.504	0.30	0.51
0.524	0.30	0.51

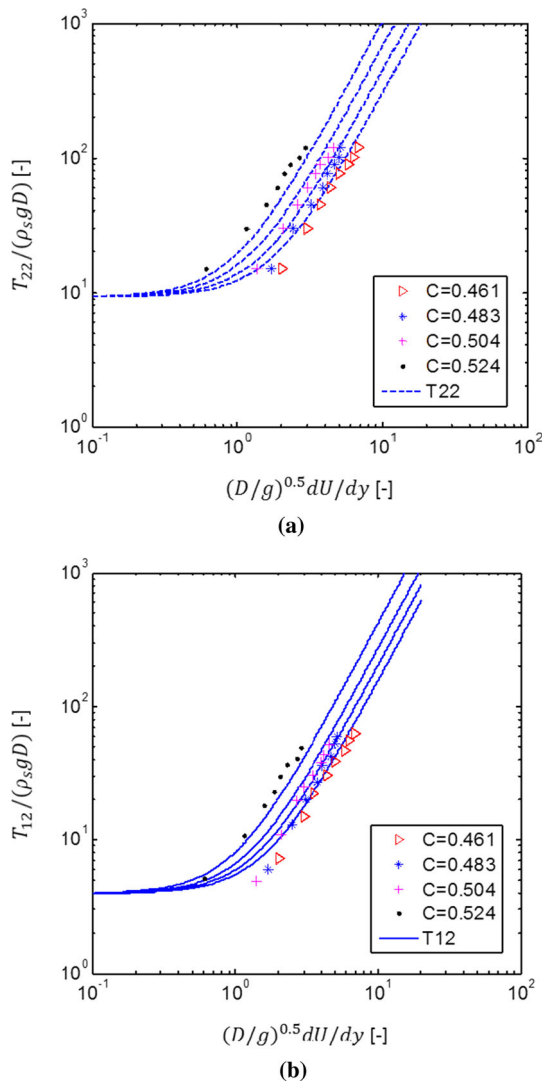


Fig. 9 Elementary modeling results for dry granular flow with different grain linear concentration: **a** normal stress and **b** shear stress. The experimental data are indicated by various symbols. The dashed lines (upper panel) denote the normal stresses, while the solid lines (lower panel) are the shear stresses, predicted by the postulated model

maximum measured volume fraction for 1.85 mm particles was reported to be 0.55 [16]. The asymptotic limit C_∞ is presumed to be approximately 0.61. The critical volume fraction is assumed to be 0.52 as a partially shearing with $C = 0.53$ was reported. The load from the upper disk, P_0 , is about 200 N/m^2 . The angle α_v is equal to the dynamic angle of repose, 28° . All the parameters are listed in Tables 3 and 4.

The predicted results are shown in Fig. 10. The predicted curves of $C = 0.51$ show a good agreement with the experimental data. The stresses of the specimen with $C = 0.49$ are slightly overestimated. Similar to the case 1, the overestimation of P_0 and T_0 may be responsible for this

Table 3 Parameters for the shear tests of 1.85 mm beads in [16]

d (mm)	C_∞ (-)	C_c (-)	ρ_s (kg/m^3)	ρ_f (kg/m^3)	μ (Pa s)	ϕ ($^\circ$)	θ ($^\circ$)
1.85	0.61	0.52	2780	1000	1.0×10^{-3}	0.59	0

Table 4 Stress ratios measured in the shear tests of 1.85 mm beads in [16]

C (-)	$\tan \alpha_v$ (-)	$\tan \alpha_i$ (-)
0.49	0.53	0.59
0.51	0.53	0.59

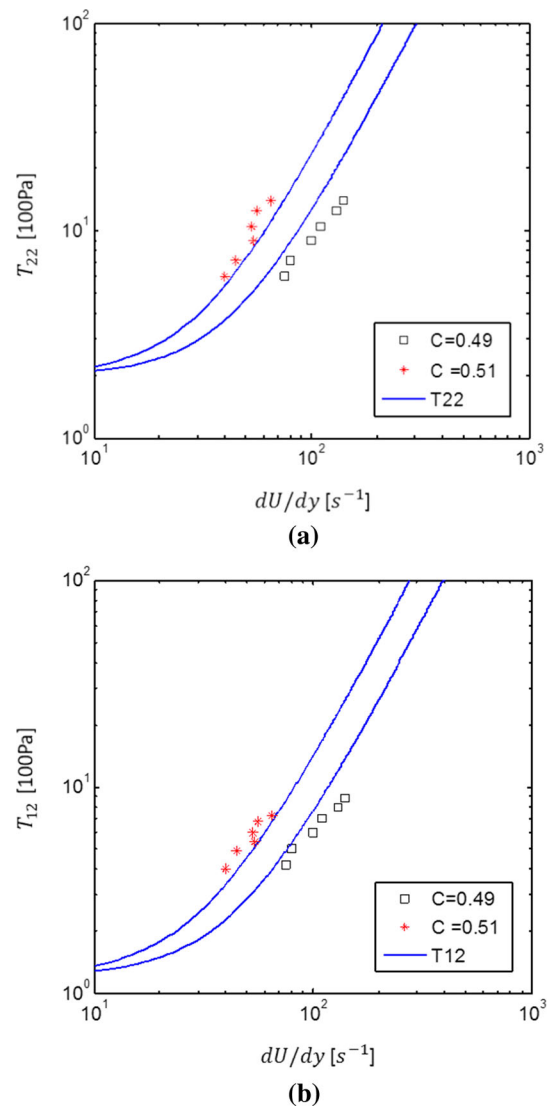


Fig. 10 Elementary modeling results for granular–water flow with different solid volume fraction: **a** normal stress and **b** shear stress. The experimental data are indicated by various symbols. The solid lines denote the normal stresses in the upper panel and the shear stresses in the lower panel, predicted by the postulated model

discrepancy. Nevertheless, the dynamic portion of the presented model is capable of describing the stress versus shear rate relation in the dense flow regime for a granular–water mixture.

6 Conclusions

A framework for the constitutive modeling of granular–fluid mixture is developed by combining a rate-independent static part with a rate-dependent rheological part in an additive form. In this framework, the effect of the prolonged contact, the viscosity of the interstitial fluid and the particle collisions are considered explicitly. The Mohr–Coulomb-type relation for the quasi-static regime and the Bagnold-type rheological model for the dense flow regime are unified in the framework to obtain a simple-shearing model which can describe the mechanical behaviors throughout the shear process from yielding to high-speed shearing. In the modified Bagnold-type model, the conversion between the so-called macro-viscous and grain-inertia regimes can be captured continuously. The critical solid volume fraction to assure the occurrence of a full shearing is taken into account. The existence of the stagnant zone is identified as the main reason for the dramatic increase in the dynamic viscosity as the solid volume fraction exceeds the critical value.

Analytical solutions for dry granular flows in three configurations, i.e., plane shear, vertical chute flow and flow on inclined plate, are derived based on the presented model. The solutions are compared with those obtained using the $\mu(I)$ model. The following observations can be made. (1) Both models show that in order to switch from the quasi-static to the gaseous regime, one can either increase the shear rate or decrease the pressure. (2) The overall phenomenological frictional coefficient is dependent on flow kinematics, material properties and boundary conditions. In both models there are lower and upper limits for this phenomenological frictional coefficient. The $\mu(I)$ model shows that the friction angle increases as the granular material approaches the gaseous regime, but does not give a physical background. The presented unified model shows that the increase in the phenomenological frictional coefficient is because of particle collisions.

The developed model is used to predict the stress–strain rate relations of two granular–fluid flows. The predicted results for specimens with different solid volume fraction show a good agreement with the experimental data in the high shear rate stage. However, when the static (or residual) normal stress in the beginning of the flowing is determined as the component of gravity or the external load on the solid phase, the total stresses in the low shear rate stage are overestimated by the new model for the relatively

loose specimens. A possible explanation is that shear softening occurs in the relatively loose specimens in the quasi-static regime and the Mohr–Coulomb model cannot capture this behavior.

Nevertheless, the unified model has some favorable distinct features. First, the quasi-static solid-like behaviors of granular materials are fully defined in the rate-independent part of the model. The modeling of the quasi-static regime, such as critical state, plastic flow and nonlinear elasticity, can be further improved by changing the static part in the unified model to more sophisticated models. Thus, the model is quite flexible for a modification. Second, granular materials in the quasi-static and dense flow regime can be described using the model uniformly, which simplifies numerical implementation. Third, the model reveals that in the dense flow regime, especially when granular materials are quite close to the gaseous regime, particle collisions contribute to a significant part of the stress.

Acknowledgements The authors wish to thank the financial support from the National Natural Science Foundation of China (Grant Numbers 51809230 and 51709230), the European Commission 7th Framework Programme Project MUMOLADE (289911), and the H2020 Marie Skłodowska-Curie Actions RISE 2017 HERCULES (778360) and FRAMED (734485).

Compliance with ethical standards

Conflict of interest The authors declare that they have no conflict of interest.

References

- Andreotti B, Forterre Y, Pouliquen O (2013) Granular media: between fluid and solid. Cambridge University Press, Cambridge
- Bagnold RA (1954) Experiments on a gravity-free dispersion of large solid spheres in a Newtonian fluid under shear. *Proc R Soc Lond A Math Phys Sci* 225:49–63
- Bagnold RA (1956) The flow of cohesionless grains in fluids. *Proc R Soc Lond A* 249:235–297
- Bailard JA (1978) An experimental study of granular fluid flow. Ph.D. thesis, University of California, La Jolla
- Bailard JA, Inman DL (1979) A reexamination of Bagnold's granular–fluid model and bed load transport equation. *J Geophys Res* 84:7827–7833
- Boyer F, Guazzelli E, Pouliquen O (2011) Unifying suspension and granular rheology. *Phys Rev Lett* 107:188301
- Calvetti F, Prisco CD, Redaelli I, Sganzerla A, Vairaktaris E (2019) Mechanical interpretation of dry granular masses impacting on rigid obstacles. *Acta Geotech* 14:1289–1305
- Chambon G, Bouvarel R, Laigle D, Naaim M (2011) Numerical simulations of granular free-surface flows using smoothed particle hydrodynamics. *J Non-Newton Fluid Mech* 166(12):698–712
- Cowin SC (1974) Constitutive relations that imply a generalized Mohr–Coulomb criterion. *Acta Mech* 20:41–46
- da Cruz F, Emam S, Prochnow M, Roux J, Chevoir F (2005) Rheophysics of dense granular material: discrete simulation of plane shear flows. *Phys Rev E* 72(2):021309

11. Eyring H, Henderson D, Stover BJ, Eyring EM (1964) *Statistical mechanics and dynamics*. Wiley, New York
12. Fang C, Wu W (2014) On the weak turbulent motions of an isothermal dry granular dense flow with incompressible grains: part I. Equilibrium turbulent closure models. *Acta Geotech* 9:725–737
13. Fang C, Wu W (2014) On the weak turbulent motions of an isothermal dry granular dense flow with incompressible grains: part II. Complete closure models and numerical simulations. *Acta Geotech* 9:739–752
14. Gudehus G (2019) Granular solid dynamics with eutaxy and hysteresis. *Acta Geotech* 10:1–15
15. Guo X, Peng C, Wu Wei, Wang Y (2016) A hypoplastic constitutive model for debris materials. *Acta Geotech* 11:1217–1229
16. Hanes DM, Inman DL (1985) Observations of rapidly flowing granular–fluid materials. *J Fluid Mech* 150:357–380
17. Hunt ML, Zenit R, Campbell CS, Brennen CE (2002) Revisiting the 1954 suspension experiments of R. A. Bagnold. *J Fluid Mech* 452:1–24
18. Iverson RM (1997) The physics of debris flows. *Rev Geophys* 35(3):245–296
19. Jop P, Forterre Y, Pouliquen O (2006) A constitutive law for dense granular flows. *Nature* 441(7094):727–730
20. Jop P, Forterre Y, Pouliquen O (2007) Initiation of granular surface flows in a narrow channel. *Phys Fluids* 19:088102
21. Mctigue DF, Savage SB (1981) Comment on A reexamination of Bagnold’s granular–fluid model and bed load transport equation by J. A. Bailard and D. L. Inman. *J Geophys Res* 86:4311–4313
22. Nedderman RM (1992) *Statics and kinematics of granular materials*. Cambridge University Press, Cambridge
23. Ness C, Sun J (2015) Flow regime transitions in dense non-Brownian suspensions: rheology, microstructural characterization, and constitutive modeling. *Phys Rev E* 91:012201
24. Peng C, Guo X, Wu Wei, Wang Y (2016) Unified modelling of granular media with smoothed particle hydrodynamics. *Acta Geotech* 11:1231–1247
25. Savage SB (1979) Gravity flow of cohesionless granular materials in chutes and channels. *J Fluid Mech* 92:53–96
26. Savage SB, Sayed M (1984) Stresses developed by dry cohesionless granular materials sheared in an annular shear cell. *J Fluid Mech* 142:391–430
27. Shibata M, Mei CC (1986) Slow parallel flows of a water–granular mixture under gravity, part I: continuum modeling. *Acta Mech* 63:179–193
28. Thomas DG (1965) Transport characteristics of suspension: VIII. A note on the viscosity of Newtonian suspensions of uniform spherical particles. *J Colloid Sci* 20:267–277
29. Wu W (2006) On high-order hypoplastic models for granular materials. *J Eng Math* 56:23–34

Publisher’s Note Springer Nature remains neutral with regard to jurisdictional claims in published maps and institutional affiliations.